ELSEVIER

www.elsevier.nl/locate/jorganchem

Journal of Organometallic Chemistry 614–615 (2000) 294–303

Journal of Organo metallic Chemistry

New Ni–Rh carbonyl clusters with unprecedented structural and electronic features: synthesis and X-ray structure of $[NEt_4]_3[Ni_{10}Rh(CO)_{19}]\cdot C_2H_5CN$, $[NMe_3CH_2Ph]_3[Ni_6Rh_3(CO)_{17}]$ and $[NEt_4]_3[Ni_9Rh_3(CO)_{22}]$

Cristina Femoni [a], Francesco Demartin [b], Maria Carmela Iapalucci [a], Alessandro Lombardi [a], Giuliano Longoni [a,*], Cristian Marin [a], Per H. Svensson [a]

[a] *Dipartimento di Chimica Fisica ed Inorganica, Universita' di Bologna, viale Risorgimento 4, 40136 Bologna, Italy*
[b] *Dipartimento di Chimica Strutturale e Stereochimica Inorganica, Universita' di Milano, via G. Venezian 21, 20133 Milan, Italy*

Received 15 June 2000

Dedicated to Professor Sheldon H. Shore on the occasion of his 70th birthday in recognition of his outstanding contributions to chemistry.

Abstract

The reaction of the $[Ni_6(CO)_{12}]^{2-}$ dianion with $[Rh(COD)Cl]_2$ (COD = cyclooctadiene) affords in sequence the new $[Ni_{10}Rh(CO)_{19}]^{3-}$ (**1**) and $[Ni_9Rh_3(CO)_{22}]^{3-}$ (**2**) trianionic clusters with good selectivity. The related $[Ni_6Rh_3(CO)_{17}]^{3-}$ (**3**) trianionic cluster has been initially isolated among the degradation products of $[Ni_9Rh_3(CO)_{22}]^{3-}$ (**2**) under carbon monoxide and has been more conveniently synthesized by condensation of $[Rh(CO)_4]^-$ with $Ni(CO)_4$ in excess. All these new bimetallic Ni–Rh carbonyl clusters have been isolated in the solid state as tetrasubstituted ammonium salts and were characterized by elemental analysis, spectroscopy and X-ray diffraction studies. The structure of $[Ni_{10}Rh(CO)_{19}]^{3-}$ (**1**) consists of a distorted and incomplete Rh-centered $Ni_9(\mu_9\text{-}Rh)$ icosahedral moiety, capped by the tenth Ni atom on one of the interlayer triangular faces. The $[Ni_{10}Rh(CO)_{19}]^{3-}$ (**1**) trianion is moderately stable to oxidation and, as inferable from IR monitoring of the resulting reaction mixture, is irreversibly degraded upon exposure to an atmosphere of carbon monoxide to a mixture of $Ni(CO)_4$, $[Rh(CO)_4]^-$ and $[Ni_5(CO)_{12}]^{2-}$. The $[Ni_9Rh_3(CO)_{22}]^{3-}$ (**2**) trianion displays a three layer metal frame identical to that previously found in the $[H_{4-x}Ni_9Pt_3(CO)_{21}]^{x-}$ ($x = 2$–4) clusters. However, it features two less valence electrons. The structure of $[Ni_6Rh_3(CO)_{17}]^{3-}$ (**3**) is closely related to that of $[Ni_9Rh_3(CO)_{22}]^{3-}$ (**2**) and may be formally derived from that of the latter by substitution of a $Ni_3(CO)_3(\mu\text{-}CO)_3$ moiety with a face bridging carbonyl group. Notably, $[Ni_6Rh_3(CO)_{17}]^{3-}$ (**3**) is isoelectronic but not isostructural with the known $[Ni_6Ir_3(CO)_{17}]^{3-}$ congener. Both $[Ni_6Rh_3(CO)_{17}]^{3-}$ (**3**) and $[Ni_9Rh_3(CO)_{22}]^{3-}$ (**2**) are readily degraded by carbon monoxide at atmospheric pressure to colourless solutions containing $Ni(CO)_4$ and $[Rh(CO)_4]^-$ mixtures. Their reaction with $[Rh(COD)Cl]_2$ leads to the previously reported $[Ni_6Rh_5(CO)_{21}]^{3-}$ trianion and other yet uncharacterised Ni–Rh carbonyl clusters. All above Ni–Rh clusters do not display protonation–deprotonation behaviour and chemically reversible redox propensity; electrochemical experiments failed in all cases to show the occurrence of electrochemically reversible redox changes. © 2000 Published by Elsevier Science B.V. All rights reserved.

Keywords: Carbonyl; Cluster; Nickel; Rhodium; X-ray structure

1. Introduction

The carbonyl cluster chemistry of both Ni and Rh has been developed to a wide extent [1,2]. In contrast, only very few bimetallic Ni–Rh carbonyl clusters have yet been reported. The only species that have so far been structurally characterized are the $[NiRh_6(CO)_{16}]^{2-}$ dianion [3], and the $[Ni_6Rh_5(CO)_{21}]^{3-}$ trianion [4]. The recent upsurge of interest in high nuclearity carbonyl clusters (see, for instance, $[Ni_{32}C_6(CO)_{36}]^{6-}$ [5], $[Ni_{16}Pd_{16}(CO)_{40}]^{4-}$ [6], $[Ni_{31}Sb_4(CO)_{40}]^{4-}$ [7], $[Pt_{38}$-

---

* Corresponding author. Fax: + 39-051-2093690.

PII: S0022-328X(00)00632-X

$(CO)_{42}]^{2-}$ [8], $[Ni_{32}Au_6(CO)_{44}]^{6-}$ [9], $[Au_6Pd_6(Pd_{6-x}Ni_x)Ni_{20}(CO)_{44}]^{6-}$ [9], $[Ni_{36}Pt_4(CO)_{45}]^{6-}$ [10], $[H_{12}Pd_{28}Pt_{13}(CO)_{27}(PPh_3)_{12}(PMe_3)]$ [11], $[Ni_9Pd_{33}(CO)_{41}(PPh_3)_6]^{4-}$ [12], $[Ni_{26}Pd_{20}(CO)_{54}]^{6-}$ [6] and $Pd_{59}(CO)_{32}(PMe_3)_{21}$ [13]), stimulated by their structural [5–13], electronic [14,15] and magnetic behavior [16], led us to investigate in detail the chemistry of Ni–Rh homoleptic carbonyl bimetallic clusters (HCBC). It was thought that the above could partially parallel the chemistry of the Ni–Pt HCBC, in view of the fact that each formal substitution of Pt with a Rh atom would only shorten the electron count by one.

We report here the synthesis, chemical and structural characterization of a series of trianionic Ni–Rh HCBC, viz. $[Ni_{10}Rh(CO)_{19}]^{3-}$ (**1**), $[Ni_9Rh_3(CO)_{22}]^{3-}$ (**2**) and $[Ni_6Rh_3(CO)_{17}]^{3-}$ (**3**), which show unprecedented structural and electronic features. Indeed, $[Ni_{10}Rh(CO)_{19}]^{3-}$ (**1**) is isoelectronic but not isostructural with the previously reported $[Ni_6Rh_5(CO)_{21}]^{3-}$ trianion [4], and represents the first example of a homoleptic carbonyl metal cluster which features a metal core based on a centred icosahedral geometry involving solely transition metal atoms [1,2]. In keeping with our working hypothesis, the $[Ni_9Rh_3(CO)_{22}]^{3-}$ (**2**) trianion displays the same metal framework of $[H_{4-x}Ni_9Pt_3(CO)_{21}]^{x-}$ ($x = 2$–4) [17], but is not isoelectronic. Finally, the structure of $[Ni_6Rh_3(CO)_{17}]^{3-}$ (**3**) is at variance from that of the $[Ni_6Ir_3(CO)_{17}]^{3-}$ [18] congener and may be described as formally deriving from that of $[Ni_9Rh_3(CO)_{22}]^{3-}$ (**2**) by substitution of a $Ni_3(CO)_3(\mu\text{-}CO)_3$ moiety with a face-bridging carbonyl group.

2. Results and discussion

2.1. Synthesis of $[Ni_{10}Rh(CO)_{19}]^{3-}$ (1), $[Ni_9Rh_3(CO)_{22}]^{3-}$ (2) and $[Ni_6Rh_3(CO)_{17}]^{3-}$ (3)

Most of our present knowledge of the chemistry of Ni–Rh HCBC is summarised in Scheme 1.

The tetraethylammonium salt of the brown $[Ni_{10}Rh(CO)_{19}]^{3-}$ (**1**) trianion separates out in good yields (> 80% based on Rh) as a waxy precipitate upon reaction in THF of $[NEt_4]_2[Ni_6(CO)_{12}]$ with $[Rh(COD)Cl]_2$ (COD = cyclooctadiene) or $[Rh(CO)_2Cl]_2$ in a 4:1 molar ratio. In both cases the only detectable by-products are $Ni(CO)_4$ and trace amounts of $[Rh(CO)_2Cl_2]^-$. $[NEt_4]_3[Ni_{10}Rh(CO)_{19}]$ is well soluble in acetone, acetonitrile, dimethylformamide (DMF) and dimethylsulfoxide (DMSO), while it is sparingly soluble or insoluble in THF, alcohol and hydrocarbons. The salt has been separated by filtration, washed with water and THF, and crystallised from acetone–isopropyl alcohol. The tetrabutylammonium salt of $[Ni_{10}Rh(CO)_{19}]^{3-}$ (**1**) has likewise been obtained and crystallised in fair yields by starting from $[NBu_4]_2[Ni_6(CO)_{12}]$. The trimethylbenzylammonium and triphenylbenzylphosphonium salts have been prepared by metathesis of $[NEt_4]_3[Ni_{10}Rh(CO)_{19}]$ with the corresponding halides. The crystals of all the above salts obtained from acetone–isopropyl alcohol or acetonitrile–diisopropyl ether mixtures were unsuitable for X-ray studies due to decay or disorder problems. Crystals suitable for X-ray studies were eventually obtained by re-crystallization of the $[NEt_4]^+$ salt of $[Ni_{10}Rh(CO)_{19}]^{3-}$ (**1**) from propionitrile and diisopropyl ether, which afforded crystals of composition $[NEt_4]_3[Ni_{10}Rh(CO)_{19}]\cdot C_2H_5CN$. In acetonitrile solution $[Ni_{10}Rh(CO)_{19}]^{3-}$ (**1**) displays infrared absorptions due to linear-, edge- and face-bridging carbonyl groups, respectively at 1990 (s), 1837 (m) and 1786 (m) cm^{-1}. Its EPR spectrum is featureless and the ^1H-NMR spectrum displays multiplets due to the protons of the tetraethylammonium cation. The diamagnetism of $[NEt_4]_3[Ni_{10}Rh(CO)_{19}]\cdot C_2H_5CN$ has been confirmed by magnetic susceptibility measurements.

The $[Ni_{10}Rh(CO)_{19}]^{3-}$ (**1**) compound is air sensitive both in solution and in the solid state. Chemical oxidation in acetonitrile with tropylium tetrafluoroborate and reduction with sodium naphthalenide in DMF, as well as protonation of $[Ni_{10}Rh(CO)_{19}]^{3-}$ (**1**) gives rise to ill-defined mixtures of products, which were not further investigated. Compound (**1**) is completely and irreversibly degraded by carbon monoxide at atmospheric pressure as shown in Scheme 1. In view of the similarities between the infrared absorptions of all reported Ni–Rh trianionic HCBC (vide infra), CO degradation reactions, carried out on small portions of the reaction solutions, have been used systematically as a diagnostic tool complementary to direct IR monitoring.

The reaction of $[Ni_{10}Rh(CO)_{19}]^{3-}$ (**1**) with an equivalent of $[Rh(CO)_2Cl]_2$ in acetonitrile leads to the $[Ni_9Rh_3(CO)_{22}]^{3-}$ (**2**) trianion. This same product has also been obtained in good yields by direct reaction in acetonitrile of $[Ni_6(CO)_{12}]^{2-}$ salts with $[Rh(COD)Cl]_2$ or $[Rh(CO)_2Cl]_2$ in a ca. 1:0.7 molar ratio. The miscellaneous tetrasubstituted ammonium salts of $[Ni_9Rh_3(CO)_{22}]^{3-}$ (**2**) have been isolated by evaporation in vacuum of the filtered reaction solutions, wash-

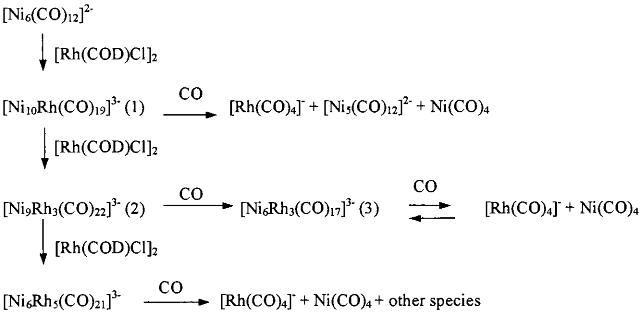

Scheme 1.

Table 1
Selected interatomic distances (Å) of $[Ni_{10}Rh(CO)_{19}]^{3-}$ (**1**) in the $[NEt_4]_3[Ni_{10}Rh(CO)_{19}]\cdot C_2H_5CN$ salt

Ni–Rh		*Ni–Ni*			
Ni(1)–Rh(1)	3.002(2)	Ni(1)–Ni(2)	2.702(2)		
Ni(2)–Rh(1)	2.589(2)	Ni(1)–Ni(3)	2.634(2)		
Ni(3)–Rh(1)	2.602(2)	Ni(1)–Ni(4)	2.459(2)		
Ni(4)–Rh(1)	2.978(2)	Ni(1)–Ni(5)	2.495(2)		
Ni(5)–Rh(1)	2.969(2)	Ni(1)–Ni(6)	2.663(2)		
Ni(6)–Rh(1)	2.641(2)	Ni(2)–Ni(3)	2.816(2)		
Ni(7)–Rh(1)	2.600(2)	Ni(2)–Ni(6)	2.459(2)		
Ni(8)–Rh(1)	2.607(2)	Ni(3)–Ni(4)	2.703(2)		
Ni(9)–Rh(1)	2.577(2)	Ni(3)–Ni(7)	2.465(2)		
		Ni(4)–Ni(5)	2.460(2)		
		Ni(4)–Ni(7)	2.695(2)		
		Ni(4)–Ni(8)	2.636(2)		
		Ni(5)–Ni(6)	2.555(2)		
		Ni(5)–Ni(8)	2.696(2)		
		Ni(5)–Ni(9)	2.735(2)		
		Ni(5)–Ni(10)	2.367(2)		
		Ni(6)–Ni(9)	2.840(2)		
		Ni(6)–Ni(10)	2.412(2)		
		Ni(7)–Ni(8)	2.772(2)		
		Ni(8)–Ni(9)	2.465(2)		
		Ni(9)–Ni(10)	2.632(2)		
Ni–C$_{(Terminal)}$		*Ni–C*$_{(Double\ bridg.)}$		*Rh–C*$_{(Double\ bridg.)}$	
Ni(1)–C(1)	1.794(13)	Ni(1)–C(14)	1.916(11)	Rh(1)–C(17)	2.010(12)
Ni(2)–C(2)	1.711(13)	Ni(1)–C(15)	1.913(11)	Rh(1)–C(18)	2.020(10)
Ni(3)–C(3)	1.753(13)	Ni(2)–C(11)	1.904(11)	Rh(1)–C(19)	2.006(12)
Ni(4)–C(4)	1.819(14)	Ni(2)–C(17)	2.035(12)		
Ni(7)–C(5)	1.753(11)	Ni(3)–C(12)	1.882(12)	Ni···C	
Ni(8)–C(6)	1.741(11)	Ni(4)–C(14)	1.893(11)	Ni(3)–C(17)	2.390(12)
Ni(9)–C(7)	1.725(12)	Ni(4)–C(16)	1.932(11)	Ni(3)–C(14)	2.494(12)
Ni(10)–C(8)	1.790(14)	Ni(5)–C(9)	1.867(13)	Ni(6)–C(15)	2.272(10)
		Ni(5)–C(16)	1.904(11)	Ni(6)–C(18)	2.437(11)
		Ni(5)–C(15)	1.944(10)	Ni(8)–C(16)	2.370(10)
		Ni(6)–C(10)	1.809(11)	Ni(8)–C(19)	2.295(11)
		Ni(6)–C(11)	1.874(10)		
		Ni(7)–C(12)	1.926(11)		
		Ni(7)–C(19)	1.977(10)		
		Ni(8)–C(13)	1.862(11)		
		Ni(9)–C(18)	1.936(11)		
		Ni(9)–C(13)	1.955(11)		
		Ni(10)–C(9)	1.832(12)		
		Ni(10)–C(10)	1.940(11)		
C–O$_{(Terminal)}$		*C–O*$_{(Double\ bridg.)}$			
C(1)–O(1)	1.131(13)	C(9)–O(9)	1.194(13)		
C(2)–O(2)	1.173(13)	C(10)–O(10)	1.137(12)		
C(3)–O(3)	1.145(13)	C(11)–O(11)	1.184(11)		
C(4)–O(4)	1.116(14)	C(12)–O(12)	1.155(12)		
C(5)–O(5)	1.116(12)	C(13)–O(13)	1.177(12)		
C(6)–O(6)	1.146(12)	C(14)–O(14)	1.175(12)		
C(7)–O(7)	1.155(12)	C(15)–O(15)	1.182(11)		
C(8)–O(8)	1.118(13)	C(16)–O(16)	1.183(12)		
		C(17)–O(17)	1.151(12)		
		C(18)–O(18)	1.187(11)		
		C(19)–O(19)	1.197(12)		

ing of the residue with water and alcohol and crystallization in acetone–isopropyl alcohol or acetonitrile–diisopropyl ether.

The red–brown $[Ni_9Rh_3(CO)_{22}]^{3-}$ (**2**) trianion displays an infrared carbonyl in acetonitrile solution at 1985 (s), 1835(ms) and 1778 (sh) cm^{-1}, and featureless

EPR and ^{1}H-NMR spectra (apart from the protons of the cation). The solid $[NMe_3CH_2Ph]_3[Ni_9Rh_3(CO)_{22}]$ salt is diamagnetic, as inferred from magnetic susceptibility measurements.

As shown in Scheme 1, $[Ni_9Rh_3(CO)_{22}]^{3-}$ (**2**) is irreversibly degraded by carbon monoxide at atmospheric pressure to a mixture of $[Rh(CO)_4]^-$ and $Ni(CO)_4$. However, upon admittance of only a limited amount of carbon monoxide the formation of the new $[Ni_6Rh_3(CO)_{17}]^{3-}$ (**3**) cluster could be unambiguously monitored by IR. Whether it arises directly from degradation of $[Ni_9Rh_3(CO)_{22}]^{3-}$ (**2**) or from subsequent condensation of $[Rh(CO)_4]^-$ with $Ni(CO)_4$ could not be safely established.

The structural similarities between $[Ni_9Rh_3(CO)_{22}]^{3-}$ (**2**) and $[H_{4-n}Ni_{12-x}Pt_x(CO)_{21}]^{n-}$ ($n = 2$–4; $x = 0$, 3) [17,19–21], and the fact that the former displays two valence electrons less than the latter, prompted a careful investigation of its redox propensity, protonation–deprotonation behaviour and hydrogenation reaction. As for $[Ni_{10}Rh(CO)_{19}]^{3-}$ (**1**), chemical oxidation in acetonitrile with tropylium tetrafluoroborate and reduction with sodium naphthalenide in DMF of $[Ni_9Rh_3(CO)_{22}]^{3-}$ (**2**) only leads to ill-defined mixtures of products. Cyclovoltammetric experiments likewise failed in disclosing the occurrence of electrochemically reversible redox changes. As shown by IR monitoring, also the reaction of $[Ni_9Rh_3(CO)_{22}]^{3-}$ (**2**) with acids results in the irreversible formation of ill-defined mixtures of oxidised products. Monitoring of the above reaction solutions by ^{1}H-FT-NMR disclosed the presence of a quartet ($J(^1H-^{103}Rh)$ 12 Hz) at -10.8 ppm, clearly indicative of a hydride coupled with three equivalent rhodium atoms. However, the signal was seldom reproducible and integration against the proton of the cation suggested that this hydride species was present only in trace amounts ($< 5\%$).

The $[Ni_6Rh_3(CO)_{17}]^{3-}$ (**3**) trianion has initially been obtained by degradation of $[Ni_9Rh_3(CO)_{22}]^{3-}$ (**2**) with the CO in defect. However, as shown in Scheme 1, $[Ni_6Rh_3(CO)_{17}]^{3-}$ (**3**) can be advantageously prepared by condensation of $[Rh(CO)_4]^-$ with $Ni(CO)_4$ in experimental conditions identical to those previously adopted for the $[Ni_6Ir_3(CO)_{17}]^{3-}$ congener [18]. The $[N(PPh_3)_2]^+$ and $[NMe_3CH_2Ph]^+$ salts of $[Ni_6Rh_3(CO)_{17}]^{3-}$ (**3**) have been isolated by evaporation in vacuum of the filtered reaction solution, washing of the residue with alcohol and crystallization in acetone–isopropyl alcohol or acetonitrile–diisopropyl ether. The brown $[Ni_6Rh_3(CO)_{17}]^{3-}$ (**3**) trianion displays an infrared carbonyl in acetonitrile solution at 1987 (s), 1834(m) and 1748(m) cm^{-1}, and featureless EPR and ^{1}H-NMR spectra (a part from the protons of the cation). Magnetic susceptibility measurements of the $[N(PPh_3)_2]_3[Ni_6Rh_3(CO)_{17}]$ salt confirmed its diamagnetism.

Both $[Ni_9Rh_3(CO)_{22}]^{3-}$ (**2**) and $[Ni_6Rh_3(CO)_{17}]^{3-}$ (**3**) further react with Rh(I) salts. The former affords the previously isolated and characterized $[Ni_6Rh_5(CO)_{21}]^{3-}$ trianion [4] in good yields, whereas the $[Ni_6Rh_3(CO)_{17}]^{3-}$ (**3**) trianion gives rise to a mixture of products comprising $[Ni_6Rh_5(CO)_{21}]^{3-}$. The nature of the latter as $[Ni_6Rh_5(CO)_{21}]^{3-}$ has been unequivocally established by X-ray studies. As shown in Scheme 1, the $[Ni_6Rh_5(CO)_{21}]^{3-}$ trianion is not stable under a carbon monoxide atmosphere and is rapidly degraded to a complex mixture of $[Rh(CO)_4]^-$, $Ni(CO)_4$ and other yet uncharacterised species.

2.2. X-ray structure of $[Ni_{10}Rh(CO)_{19}]^{3-}$ (1), $[Ni_9Rh_3(CO)_{22}]^{3-}$ (2) and $[Ni_6Rh_3(CO)_{17}]^{3-}$ (3)

2.2.1. $[NEt_4]_3[Ni_{10}Rh(CO)_{19}]\cdot C_2H_5CN$

The unit cell of this compound contains cluster trianions, $[NEt_4]^+$ cations and propionitrile molecules sepa-

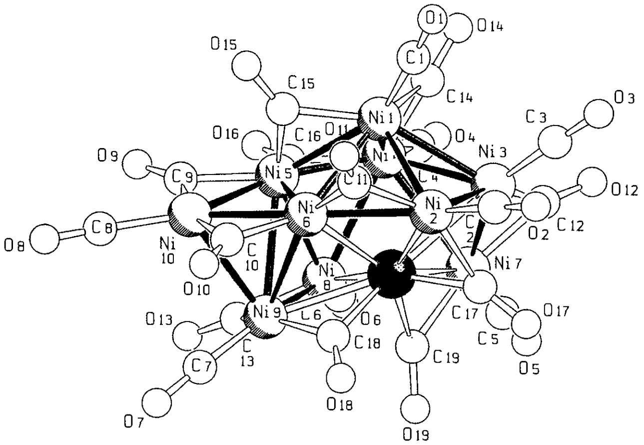

Fig. 1. Drawing of the $[Ni_{10}Rh(CO)_{19}]^{3-}$ (**1**) trianion (the unique rhodium atom is shown as a blackened sphere).

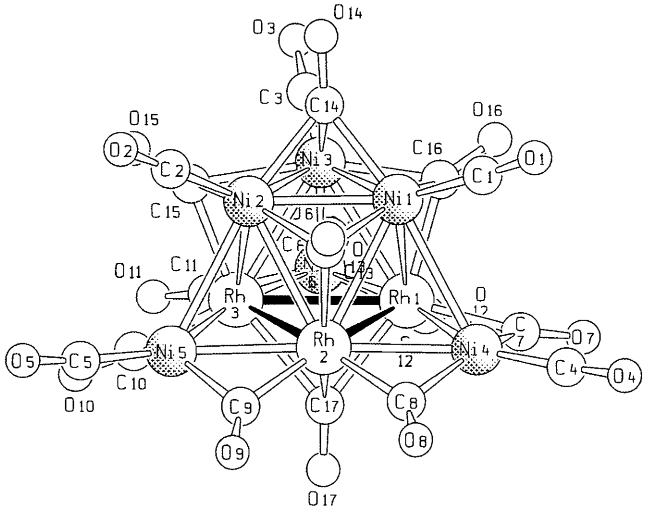

Fig. 2. Drawing of the $[Ni_6Rh_3(CO)_{17}]^{3-}$ (**3**) trianion.

Table 2
Selected interatomic distances (Å) of $[Ni_6Rh_3(CO)_{17}]^{3-}$ (**3**) in $[NMe_3CH_2Ph]_3[Ni_6Rh_3(CO)_{17}]$

M–M$_{(Intralayer)}$		*M–M*$_{(Interlayer)}$			
Ni(1)–Ni(2)	2.505(2)	Ni(1)–Ni(4)	2.821(2)		
Ni(1)–Ni(3)	2.468(1)	Ni(2)–Ni(5)	2.804(2)		
Ni(2)–Ni(3)	2.494(1)	Ni(3)–Ni(6)	2.773(2)		
Rh(1)–Rh(2)	2.845(1)	Rh(1)–Ni(1)	2.727(1)		
Rh(1)–Rh(3)	2.863(2)	Rh(1)–Ni(3)	2.707(1)		
Rh(2)–Rh(3)	2.865(1)	Rh(2)–Ni(1)	2.758(1)		
Rh(1)–Ni(4)	2.553(1)	Rh(2)–Ni(2)	2.733(1)		
Rh(1)–Ni(6)	2.546(1)	Rh(3)–Ni(2)	2.733(1)		
Rh(2)–Ni(4)	2.569(1)	Rh(3)–Ni(3)	2.678(1)		
Rh(2)–Ni(5)	2.564(1)				
Rh(3)–Ni(5)	2.531(1)				
Rh(3)–Ni(6)	2.546(1)				
M–C$_{(Terminal)}$		M–C$_{(Double\ bridg.)}$		M–C$_{(Triple\ bridg.)}$	
Ni(1)–C(1)	1.756(6)	Rh(1)–C(7)	2.005(6)	Rh(1)–C(16)	2.104(6)
Ni(2)–C(2)	1.748(6)	Rh(1)–C(12)	1.936(7)	Rh(1)–C(17)	2.211(6)
Ni(3)–C(3)	1.739(7)	Rh(2)–C(8)	1.981(6)	Rh(2)–C(13)	2.132(6)
Ni(4)–C(4)	1.722(6)	Rh(2)–C(9)	1.970 (6)	Rh(2)–C(17)	2.181(7)
Ni(5)–C(5)	1.744(7)	Rh(3)–C(10)	1.958(6)	Rh(3)–C(15)	2.033(6)
Ni(6)–C(6)	1.723(8)	Rh(3)–C(11)	1.996(7)	Rh(3)–C(17)	2.316(6)
		Ni(4)–C(7)	1.942(6)	Ni(1)–C(13)	2.108(7)
		Ni(4)–C(8)	1.977(6)	Ni(1)–C(14)	2.005(6)
		Ni(5)–C(9)	1.924(6)	Ni(1)–C(16)	2.167(7)
		Ni(5)–C(10)	1.974(7)	Ni(2)–C(13)	2.055(7)
		Ni(6)–C(11)	1.936(6)	Ni(2)–C(14)	2.086(6)
		Ni(6)–C(12)	1.968(6)	Ni(2)–C(15)	2.035(7)
				Ni(3)–C(14)	2.017(6)
				Ni(3)–C(15)	2.196(6)
				Ni(3)–C(16)	2.026(6)
C–O$_{(Terminal)}$		*C–O*$_{(Double\ bridg.)}$		*C–O*$_{(Triple\ bridg.)}$	
O(1)–C(1)	1.148(8)	O(7)–C(7)	1.147(6)	O(13)–C(13)	1.204(8)
O(2)–C(2)	1.154(8)	O(8)–C(8)	1.154(9)	O(14)–C(14)	1.186(7)
O(3)–C(3)	1.138(9)	O(9)–C(9)	1.172(9)	O(15)–C(15)	1.198(7)
O(4)–C(4)	1.160(7)	O(10)–C(10)	1.143(8)	O(16)–C(16)	1.188(7)
O(5)–C(5)	1.136(8)	O(11)–C(11)	1.154(8)	O(17)–C(17)	1.157(8)
O(6)–C(6)	1.151(9)	O(12)–C(12)	1.156(8)		

rated by normal van der Waals contacts. The structure of the trianion consists of a Rh-centered $Ni_9(\mu_9\text{-}Rh)$ incomplete icosahedral moiety, capped on one interlayer triangular face by the tenth nickel atom (Ni(10) in Fig. 1). The missing three vertex of the icosahedron and the capping Ni(10) atom give rise to complete disruption of the icosahedral symmetry. This metal atom assembly is completely unprecedented in transition metal clusters, even if several examples of undecanuclear carbonyl metal clusters have previously been characterized, e.g. $[Rh_{11}(CO)_{23}]^{3-}$ [22], $[Os_{11}C(CO)_{27}]^{2-}$ [23], $[Co_{11}C_2(CO)_{22}]^{3-}$ [24], $[PtRh_{10}N(CO)_{21}]^{3-}$ [25], $[Pt_2Rh_9(CO)_{22}]^{3-}$ [26] and $[Ni_6Rh_5(CO)_{21}]^{3-}$ [4]. Interestingly, the structure of the Rh-centered $Ni_9(\mu_9\text{-}Rh)$ incomplete icosahedral moiety stands to the $[B_9H_{14}]^-$ arachno-borane [27], as the E-centred $[Ni_{12}(\mu_{12}\text{-}E)(CO)_{22}]^{2-}$ (E = Ge, Sn) [28] and $[Rh_{12}(\mu_{12}\text{-}Sb)(CO)_{27}]^{3-}$ [29] stand to the $[B_{12}H_{12}]^{2-}$ *closo*-borane [27]. To our knowledge $[Ni_{10}Rh(CO)_{19}]^{3-}$ (**1**) is the first carbonyl cluster only comprising of transition metal atoms in its core which shows an analogy with icosahedral boranes. The Ni–Ni distances (Table 1) of the incomplete icosahedral moiety are spread over a range wider than that observed in $[Ni_{12}(\mu_{12}\text{-}E)(CO)_{22}]^{2-}$ (E = Sn, Ge), but narrower than the one observed in $[Ni_{15}(\mu_{12}\text{-}Sb)(CO)_{24}]^{2-}$ [30], where complete icosahedral frameworks were present. The Ni–Rh distances are spread in the 2.577(**2**)–3.002(**2**) range and their average is larger than the average Ni–Sn and Ni–Sb distances{2.73 vs. 2.64 and 2.60 Å found in $[Ni_{15}(\mu_{12}\text{-}Sb)(CO)_{24}]^{2-}$ and $[Ni_{12}(\mu_{12}\text{-}Sn)(CO)_{22}]^{2-}$, respectively}. The Ni(10) cap is unsymmetrical and displays two short (Ni(5)–Ni(10) and Ni(6)–Ni(10), mean value 2.39 Å) and one long (Ni(9)–Ni(10) 2.632(2) Å) Ni–Ni bonds. The 19 CO ligands are bonded as follows: 8 are terminal and 11 are edge bridging. As shown in Table 1, six of the edge-bridging carbonyl groups lean toward a third atom with contacts in the 2.27–2.49 Å range and may be considered as incipient face bridging ligands. The above carbonyl stereochemistry is only in partial agreement with the solution IR spectrum, which shows two distinct absorptions for edge- and face-bridges. Notably, the two Ni(5) and Ni(6) atoms, belonging to the Ni_5 ring of the Ni_9Rh moiety and connected by short bond to the Ni(10) cap, do not bind terminal carbonyl groups. The unique rhodium atom (shown as a blackened sphere in Fig. 1) is coordinated by three edge-bridging ligands.

It seems conceivable to suggest that the unprecedented structure of $[Ni_{10}Rh(CO)_{19}]^{3-}$ (**1**) is triggered both by the size of the encapsulated Rh atom and its affinity for carbon monoxide. In the series of icosahedral or incomplete icosahedral $[Ni_{12}(\mu_{12}\text{-}Ge)(CO)_{22}]^{2-}$, $[Ni_{12}(\mu_{12}\text{-}Sn)(CO)_{22}]^{2-}$, $[Ni_{15}(\mu_{12}\text{-}Sb)(CO)_{24}]^{2-}$ and $[Ni_{10}Rh(CO)_{19}]^{3-}$ (**1**) the observed radius of the interstitial or semi-interstitial E hetero-atom ($\text{Ni–E}_{av.} - 1/2\text{Ni–Ni}_{av.}$) is 1.22, 1.26, 1.31 and 1.43 Å and involves a progressive distortion of the icosahedral cage up to disruption. The shrinking or swelling of the E atom, with respect to its covalent size, are probably a consequence of the electronegativity difference between E and the surrounding nickel carbonyl cage.

2.2.2. $[NMe_3CH_2Ph]_3[Ni_6Rh_3(CO)_{17}]$

The unit cell of this compound contains cluster trianions and $[NMe_3CH_2Ph]^+$ cations separated by normal van der Waals contacts. A view of the $[Ni_6Rh_3(CO)_{17}]^{3-}$ (**3**) trianion is shown in Fig. 2 and the most relevant bond contacts are collected in Table 2. The two-layer metal frame of $[Ni_6Rh_3(CO)_{17}]^{3-}$ (**3**) derives from the condensation of a planar Ni_3Rh_3 ν_2-triangle with a Ni_3 triangular moiety, so as to give rise to a Ni_3Rh_3 trigonal antiprism capped onto three alternate triangular faces. To our knowledge, only the bimetallic $[Ag_6Fe_3(CO)_{12}(PPh_2)_3CH]$ displays a related two-layer frame [31], whereas all remaining enneanuclear metal carbonyl clusters, including the $[Ni_6Ir_3(CO)_{17}]^{3-}$ congener, show three-layer metal frames based on face-sharing bioctahedra (e.g. $[Rh_9(CO)_{19}]^{3-}$ [32], $[Ir_9(CO)_{20}]^{3-}$ and $[HIr_9(CO)_{19}]^{4-}$ [33]), face-sharing trigonal prisms (e.g. $[Pt_9(CO)_{18}]^{2-}$ [34]), face-sharing trigonal prism and antiprism (e.g. $[Ni_9(CO)_{18}]^{2-}$ [35]) or capped square antiprism as $[Rh_9P(CO)_{21}]^{3-}$ [36].

The carbonyl stereochemistry of $[Ni_6Rh_3(CO)_{17}]^{3-}$ (**3**) comprises six terminal groups (one per each nickel atom), six edge-bridging carbonyls spanning the six Ni–Rh bonds of the Ni_3Rh_3 ν_2-triangle, and five face-bridging carbonyl ligands capping the two unique Ni_3 and Rh_3 faces and three Ni_2Rh triangles. This stereochemistry is maintained in solution as indicated by the presence of IR absorptions in the terminal, edge- and face-bridging region, and is probably at the origin of the structural differences between the $[Ni_6M_3(CO)_{17}]^{3-}$ (M = Rh, Ir) congeners. Indeed, the formal conversion of the metal frame of $[Ni_6Rh_3(CO)_{17}]^{3-}$ (**3**) into the face-sharing bioctahedral frame of $[Ni_6Ir_3(CO)_{17}]^{3-}$ could be formally achieved by breaking the three interlayer Ni(1)–Ni(4), Ni(2)–Ni(5) and Ni(3)–Ni(6) bonds and flipping down the three Ni(4), Ni(5) and Ni(6) atoms to generate a third layer. However, this metal rearrangement implies the loss of the Rh_3 face-bridging site and the probable conversion of the face-bridging carbonyls capping the Ni_2Rh faces into edge-bridging ligands. The different propensity of Rh and Ir for face-bridging carbonyl groups [2] could drive the two $[Ni_6M_3(CO)_{17}]^{3-}$ (M = Rh, Ir) congeners to adopt their different structures.

2.2.3. $[NEt_4]_3[Ni_9Rh_3(CO)_{22}]$

The asymmetric unit of $[NEt_4]_3[Ni_9Rh_3(CO)_{22}]$ consists of a $[Ni_9Rh_3(CO)_{22}]^{3-}$ (**2**) anion, two $[NEt_4]^+$ cations in a general position of the space group and two additional half cations located on crystallographic two-fold axes. All four $[NEt_4]^+$ cations are affected by high thermal motion and two among them are partially disordered and some of their atoms have not been located. In spite of that, the charge of the anion has been unambiguously established. A view of the $[Ni_9Rh_3(CO)_{22}]^{3-}$ (**2**) anion is shown in Fig. 3; the most relevant bond contacts are collected in Table 3. Its three-layer metal frame represents a chunk of the hexagonal close-packed metal lattice and is identical to that displayed by the $[H_{4-n}Ni_9M_3(CO)_{21}]^{n-}$ (M = Ni, Pt) derivative. The additional carbonyl group face-bridges one of the two $Ni_3(CO)_3(\mu\text{-}CO)_3$ triangular moieties and pushes into a face-bridging coordination

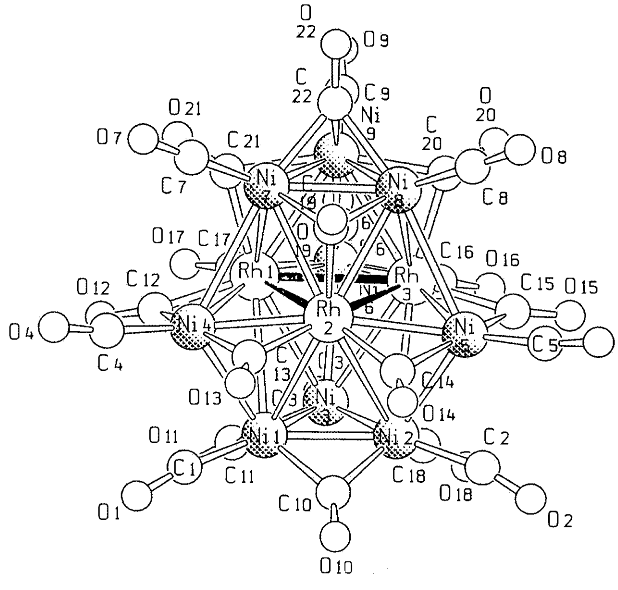

Fig. 3. Drawing of the $[Ni_9Rh_3(CO)_{22}]^{3-}$ (**2**) trianion.

Table 3
Selected interatomic distances (Å) of $[Ni_9Rh_3(CO)_{22}]^{3-}$ (**2**) in $[NEt_4]_3[Ni_9Rh_3(CO)_{22}]$

M–M$_{(Interlayer)}$		*M–M*$_{(Intralayer)}$			
Rh(1)–Ni(1)	3.054(2)	Rh(1)–Rh(2)	2.918(1)		
Rh(1)–Ni(3)	2.954(2)	Rh(1)–Rh(3)	2.926(1)		
Rh(1)–Ni(7)	2.705(2)	Rh(1)–Ni(4)	2.559(2)		
Rh(1)–Ni(9)	2.707(2)	Rh(1)–Ni(6)	2.555(2)		
Rh(2)–Ni(1)	2.952(2)	Rh(2)–Rh(3)	2.925(1)		
Rh(2)–Ni(2)	3.059(2)	Rh(2)–Ni(4)	2.559(2)		
Rh(2)–Ni(7)	2.711(2)	Rh(2)–Ni(5)	2.561(2)		
Rh(2)–Ni(8)	2.710(2)	Rh(3)–Ni(5)	2.553(2)		
Rh(3)–Ni(2)	2.954(2)	Rh(3)–Ni(6)	2.556(2)		
Rh(3)–Ni(3)	3.058(2)	Ni(1)–Ni(2)	2.449(2)		
Rh(3)–Ni(8)	2.707(2)	Ni(1)–Ni(3)	2.447(2)		
Rh(3)–Ni(9)	2.709(2)	Ni(2)–Ni(3)	2.448(2)		
Ni(1)–Ni(4)	2.697(3)	Ni(7)–Ni(8)	2.455(2)		
Ni(2)–Ni(5)	2.697(3)	Ni(7)–Ni(9)	2.448(2)		
Ni(3)–Ni(6)	2.701(3)	Ni(8)–Ni(9)	2.449(2)		
Ni(4)–Ni(7)	2.952(3)				
Ni(5)–Ni(8)	2.946(3)				
Ni(6)–Ni(9)	2.937(3)				
M–C$_{(Terminal)}$		*M–C*$_{(Double\ bridg.)}$		*M–C*$_{(Triple\ bridg.)}$	
Ni(1)–C(1)	1.795(13)	Rh(1)–C(12)	1.969(13)	Rh(1)–C(21)	2.021(15)
Ni(2)–C(2)	1.815(13)	Rh(1)–C(17)	1.985(11)	Rh(2)–C(19)	2.030(16)
Ni(3)–C(3)	1.766(11)	Rh(2)–C(13)	2.023(12)	Rh(3)–C(20)	2.084(19)
Ni(4)–C(4)	1.802(17)	Rh(2)–C(14)	2.016(13)	Ni(7)–C(19)	2.061(12)
Ni(5)–C(5)	1.715(14)	Rh(3)–C(15)	1.988(14)	Ni(7)–C(21)	1.988(10)
Ni(6)–C(6)	1.790(15)	Rh(3)–C(16)	1.946(11)	Ni(7)–C(22)	2.002(16)
Ni(7)–C(7)	1.767(15)	Ni(1)–C(10)	1.935(13)	Ni(8)–C(19)	2.027(13)
Ni(8)–C(8)	1.732(14)	Ni(1)–C(11)	1.915(11)	Ni(8)–C(20)	2.064(12)
Ni(9)–C(9)	1.781(19)	Ni(2)–C(10)	1.919(13)	Ni(8)–C(22)	2.011(16)
		Ni(2)–C(18)	1.938(12)	Ni(9)–C(20)	2.049(13)
		Ni(3)–C(11)	1.912(13)	Ni(9)–C(21)	2.064(13)
		Ni(3)–C(18)	1.978(14)	Ni(9)–C(22)	2.012(14)
		Ni(4)–C(12)	1.959(11)		
		Ni(4)–C(13)	1.955(11)		
		Ni(5)–C(14)	2.020(12)		
		Ni(5)–C(15)	1.967(12)		
		Ni(6)–C(16)	1.959(13)		
		Ni(6)–C(17)	1.939(13)		
C–O$_{(Terminal)}$		*C–O*$_{(Double\ bridg.)}$		*C–O*$_{(Triple\ bridg.)}$	
O(1)–C(1)	1.124(17)	O(10)–C(10)	1.117(17)	O(19)–C(19)	1.174(14)
O(2)–C(2)	1.103(17)	O(11)–C(11)	1.148(15)	O(20)–C(20)	1.149(17)
O(3)–C(3)	1.131(15)	O(12)–C(12)	1.154(15)	O(21)–C(21)	1.186(16)
O(4)–C(4)	1.129(21)	O(13)–C(13)	1.124(14)	O(22)–C(22)	1.144(23)
O(5)–C(5)	1.130(18)	O(14)–C(14)	1.110(15)		
O(6)–C(6)	1.095(18)	O(15)–C(15)	1.123(17)		
O(7)–C(7)	1.120(20)	O(16)–C(16)	1.151(16)		
O(8)–C(8)	1.138(19)	O(17)–C(17)	1.130(15)		
O(9)–C(9)	1.107(23)	O(18)–C(18)	1.123(17)		

the three formerly edge-bridging carbonyl groups. Similar capping of the second $Ni_3(CO)_3(\mu\text{-}CO)_3$ moiety with a CO group would result in short C···C non-bonding contact and seems to be both sterically and electronically unfavourable, even if the $[Ni_9Rh_3(CO)_{22}]^{3-}$ (**2**) cluster ends up in having two less valence electrons than the isostructural $[H_{4-n}Ni_9M_3(CO)_{21}]^{n-}$ (M = Ni, Pt) derivatives.

The overall structure of $[Ni_9Rh_3(CO)_{22}]^{3-}$ (**2**) is also closely related to that of $[Ni_6Rh_3(CO)_{17}]^{3-}$ (**3**) and derives from the latter by formal substitution of a face bridging carbonyl group with a $Ni_3(CO)_3(\mu\text{-}CO)_3$ moiety. The donor–acceptor bonding behaviour of the $M_3L_3(\mu\text{-}CO)_3$ (M = Pd, Pt; L = phosphine) and $M_3(CO)_3(\mu\text{-}CO)_3$ (M = Ni, Pt) moieties have been reviewed [37]. The donor capacity of the $M_3(CO)_3(\mu\text{-}CO)_3$

(M = Ni, Pt) fragment is not yet documented. Their acceptor behaviour is suggested by the existence, for instance, of $[M_3(CO)_3(\mu\text{-}CO)_3]_2^{2-}$ (M = Ni, Pt) [34,38] clusters, which were interpreted to arise from electron–donation from a strong $[M_3(CO)_3(\mu\text{-}CO)_3]^{2-}$ Lewis base to a $M_3(CO)_3(\mu\text{-}CO)_3$ moiety acting as a Lewis acid [37]. The $[Pt_3(CO)_3(\mu\text{-}CO)_3]^{2-}$ Lewis base has been recently characterized by LXR and NMR studies, whereas the related $[Ni_3(CO)_3(\mu\text{-}CO)_3]^{2-}$ species was not observed [39]. The structural relationship between $[Ni_6Rh_3(CO)_{17}]^{3-}$ (**3**) and $[Ni_9Rh_3(CO)_{22}]^{3-}$ (**2**) could be taken as proof of the donor ability of the $Ni_3(CO)_3(\mu\text{-}CO)_3$ fragment. EHMO calculations with CACAO [40] implements the above suggestion. A simplified drawing of the LUMO of the $[Ni_6Rh_3(CO)_{16}]^{3-}$ fragment is shown in Fig. 4a. This has a suitable symmetry to interact with the σ lone pair of carbon monoxide to give $[Ni_6Rh_3(CO)_{17}]^{3-}$ (**3**), as well as the HOMO of the $Ni_3(CO)_3(\mu\text{-}CO)_3$ fragment (Fig. 4b) to give $[Ni_9Rh_3(CO)_{22}]^{3-}$ (**2**).

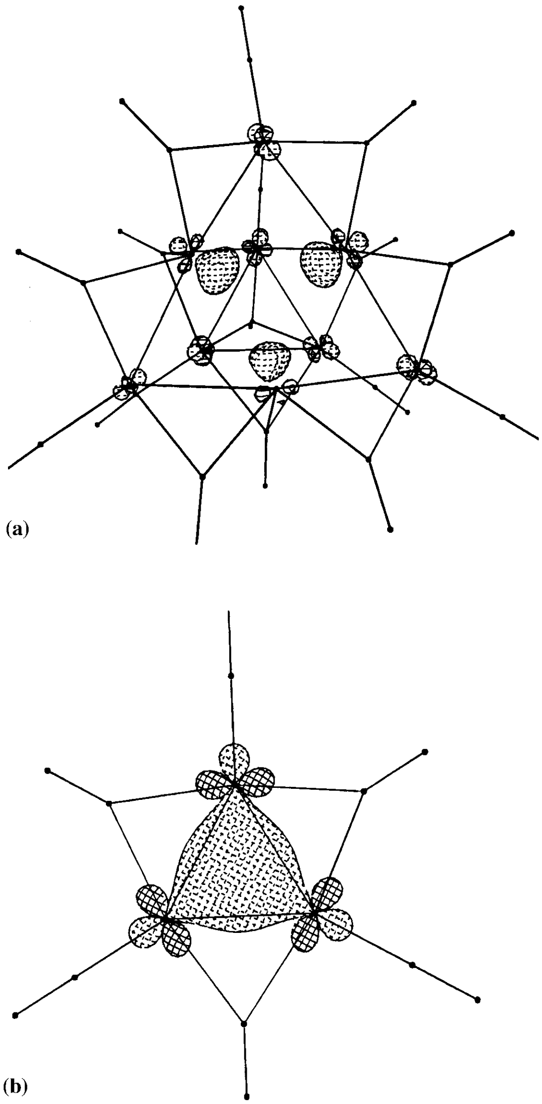

Fig. 4. The LUMO of the $[Ni_6Rh_3(CO)_{16}]^{3-}$ (a) and the HOMO of the $Ni_3(CO)_3(\mu\text{-}CO)_3$ (b) fragments oriented along the C_3 axis.

Finally, the reported results unequivocally confirm the relevance of the nature of the particular metals associated in the HCBC in determining the electronic and structural features of the bimetallic clusters.

3. Experimental

All reactions including sample manipulations were carried out using standard Schlenk techniques under nitrogen and in carefully dried solvents. The $[Ni_6(CO)_{12}]^{2-}$ salts have been prepared according to the literature [41]. Analyses of Ni and Rh were performed by atomic absorption on a Pye-Unicam instrument. Infrared spectra were recorded on a Perkin–Elmer 1605 interferometer using CaF_2 cells. EPR spectra have been recorded on a Bruker ESP 300E spectrometer and magnetic moments have been measured with a Sherwood magnetic balance. Proton NMR spectra have been recorded on a Varian Gemini 300 MHz instrument.

3.1. Synthesis of $[NEt_4]_3[Ni_{10}Rh(CO)_{19}]$

$[NEt_4]_2[Ni_6(CO)_{12}]$ (5.08 g, 5.36 mmol) was dissolved in anhydrous THF (50 ml) in a 250 ml flask under nitrogen atmosphere. A solution of $[Rh(COD)Cl]_2$ (1.33 g, 2.7 mmol) in anhydrous THF (30 ml) was added in portions under stirring over a period of 2 h, while continually removing the developing carbon monoxide with a slow stream of nitrogen. The resulting brown suspension was filtered and the brown precipitate was washed with water (30 ml), THF (20 ml) and methanol (30 ml), and extracted with acetone (50 ml). The acetone solution was concentrated to ca. 30 ml and precipitated by diffusion of isopropyl alcohol (50 ml) to give $[NEt_4]_3[Ni_{10}Rh(CO)_{19}]$ (2.31 g) as black crystals. Analytical results: Found: C, 32.25; H, 3.81; N, 2.47; Ni, 36.1; Rh, 6.1. Calc. for $[NEt_4]_3[Ni_{10}Rh(CO)_{19}]$: C, 32.01; H, 3.72; N, 2.61; Ni, 36.42; Rh, 6.38%.

Crystals of $[NEt_4]_3[Ni_{10}Rh(CO)_{19}]\cdot C_2H_5CN$ suitable for X-ray studies were obtained from the above by recrystallization from propionitrile and diisopropyl ether.

3.2. Synthesis of $[NMe_3CH_2Ph]_3[Ni_6Rh_3(CO)_{17}]$

$Ni(CO)_4$ (2 ml) and a solution of $Na[Rh(CO)_4]$ in THF (30 ml) were placed in a flask equipped with a condenser cooled at − 20°C. The mixture was warmed at 50°C and stirred under a slow stream of nitrogen for 8 h. The resulting red–brown solution was evaporated to dryness. The residue was dissolved in methanol (30 ml) and precipitated by addition of $[NMe_3CH_2Ph]Cl$ in water (30 ml). The microcrystalline precipitate was filtered off, washed with isopropyl alcohol and dried in vacuo. Extraction of the precipitate with acetone (30 ml) and precipitation by diffusion of isopropyl alcohol (70 ml) gave $[NMe_3CH_2Ph]_3[Ni_6Rh_3(CO)_{17}]$ (0.76 g) as black crystals. Anal. Found: C, 35.29; H, 3.26; N, 2.47; Ni, 22.0; Rh, 19.6. Calc. for $[NMe_3CH_2Ph]_3[Ni_6Rh_3(CO)_{17}]$: C, 35.54; H, 3.02; N, 2.65; Ni, 22.20; Rh, 19.45%.

3.3. Synthesis of $[NEt_4]_3[Ni_9Rh_3(CO)_{22}]$

$[NEt_4]_2[Ni_6(CO)_{12}]$ (3.38 g, 3.56 mmol) was dissolved in anhydrous acetonitrile (40 ml) in a 250-ml flask under a nitrogen atmosphere. A solution of $[Rh(COD)Cl]_2$ (1.22 g, 2.5 mmol) in anhydrous acetonitrile (30 ml) was added in portions under stirring over a period of 6 h, while continually removing the developing carbon monoxide with a slow stream of nitrogen. The resulting brown suspension was filtered and the solution was evaporated to dryness. The brown residue was washed with water (30 ml), THF (20 ml) and methanol (30 ml). The residue was extracted in acetone (30 ml) and precipitated by diffusion of isopropyl alcohol (50 ml) to give $[NEt_4]_3[Ni_9Rh_3(CO)_{22}]$ (0.74 g) as black crystals. Anal. Found: C, 30.05; H, 3.43; N, 2.18; Ni, 28.3; Rh, 16.4. Calc. for $[NEt_4]_3[Ni_9Rh_3(CO)_{22}]$: C, 29.95; H, 3.26; N, 2.28; Ni, 28.67; Rh, 16.75%.

3.4. X-ray data collection and structure determination of $[NEt_4]_3[Ni_{10}Rh(CO)_{19}]\cdot C_2H_5CN$, $[NMe_3CH_2Ph]_3[Ni_6Rh_3(CO)_{17}]$ and $[NEt_4]_3[Ni_9Rh_3(CO)_{22}]$

A summary of the crystallographic data and structure refinement is reported in Table 4. Data collection for $[NEt_4]_3[Ni_{10}Rh(CO)_{19}]\cdot C_2H_5CN$ was performed at room temperature on a Bruker SMART 2000 diffractometer equipped with a CCD detector, with the generator working at 50 kV and 40 mA. Those for $[NMe_3CH_2Ph]_3[Ni_6Rh_3(CO)_{17}]$ and $[NEt_4]_3[Ni_9Rh_3(CO)_{22}]$ have been carried out on a Siemens SMART diffractometer equipped with a CCD area detector, with the generator working at 45 kV and 40 mA. Cell parameters and orientation matrix were obtained from least-squares refinement on the reflections measured in three different sets of 15 frames each, in the range $0 < \theta < 25°$. The intensity data were collected in the full sphere (ω scan method); 2100 frames (20 s per frame; $\Delta\omega = 0.3°$) were collected; the first 100 frames, were recollected to have a monitoring of crystal decay, which was not observed; an absorption correction was applied (SADABS) [42]. The structures were solved by direct methods (SIR-97 [43]) and refined with full-matrix-block least squares (SHELX-97 [44]) on the basis of independent reflections with $I > 2\sigma(I)$; anisotropic temperature factors were assigned to all non-hydrogen atoms. With the only exception of $[NEt_4]_3[Ni_9Rh_3(CO)_{22}]$, where

Table 4
Crystallographic data

Compound	$[NEt_4]_3[Ni_{10}Rh(CO)_{19}]\cdot C_2H_5CN$	$[NMe_3CH_2Ph]_3[Ni_6Rh_3(CO)_{17}]$	$[NEt_4]_3[Ni_9Rh_3(CO)_{22}]$
Formula weight (amu)	1660.0	1587.9	1844.0
Space group	$P\bar{1}$ (*n*.2)	$P2_1/c$ (*n* 14)	$C2/c$ (*n* 15)
a (Å)	12.192(2)	12.068(6)	33.257(3)
b (Å)	12.699(2)	14.959(7)	22.673(3)
c (Å)	22.387(3)	30.617(15)	20.116(2)
α (°)	87.26(1)	90	90
β (°)	87.48(1)	94.48(1)	116.30(1)
γ (°)	63.51(2)	90	90
V (Å^3)	3098(1)	5510(6)	13598(7)
Z	2	4	8
Crystal dimensions	$0.12 \times 0.14 \times 020$ mm	$0.10 \times 0.10 \times 0.12$ mm	$0.10 \times 0.15 \times 0.18$ mm
Radiation (Å)	Graphite monochromatized Mo–K$_\alpha$ (0.71073)		
μ (Mo–K$_\alpha$) (cm^{-1})	32.90	29.45	32.03
θ Range (°)	1.8–25.0	1.3–29.4	1.1–26.9
Independent reflections	10892	13403	12917
Observed reflections [$I>2\sigma(I)$]	5026	7214	6145
Transmission factors	0.60–0.72	0.69–1.00	0.50–1.00
Parameters refined	686	685	731
Final R and wR_2 [a]	0.062, 0.147	0.046, 0.124	0.069, 0.223
Largest difference peak and hole (e·Å^{-3})	2.33, −1.29	0.98, −1.50	1.12, −0.82

[a] $R = [\Sigma(|F_o| - |F_c|)/\Sigma|F_o|] wR_2 = \{\Sigma[w(F_o^2 - F_c^2)^2]/\Sigma[w(F_o^2)^2]\}^{1/2}$.

quite high displacement parameters were observed for the atoms of the cations, the hydrogen atoms were included in the structure model riding on their carbon atoms.

4. Supplementary material

Crystallographic data for the structural analysis have been deposited with the Cambridge Crystallographic Data Centre, CCDC no. 143600 for $[NEt_4]_3[Ni_{10}Rh(CO)_{19}]\cdot C_2H_5CN$, no. 143601 for $[NMe_3CH_2Ph]_3[Ni_6Rh_3(CO)_{17}]$ and no. 143602 for $[NEt_4]_3[Ni_9Rh_3(CO)_{22}]$. Copies of this information may be obtained free of charge from: The Director, CCDC, 12 Union Road, Cambridge, CB2 1EZ, UK (Fax: +44-1223-336033; e-mail: deposit@ccdc.cam.ac.uk or www: http://www.ccdc.cam.ac.uk).

Acknowledgements

We thank the University of Bologna and the MURST (Cofin-98) for a grant.

References

[1] G. Longoni, M.C. Iapalucci, in: G. Schmid (Ed.), Clusters and Colloids — From Theory to Applications, VCH, Weinheim, 1994, pp. 89–177 (Chapter 3.2).

[2] A. Ceriotti, R. Della Pergola, L. Garlaschelli, in: L.J. De Jongh (Ed.), Physics and Chemistry of Metal Cluster Compounds, Kluwer, The Netherlands, 1994, pp. 41–106.

[3] A. Fumagalli, G. Longoni, P. Chini, A. Albinati, S. Bruckner, J. Organomet. Chem. 202 (1980) 329.

[4] D.A. Nagaki, J.V. Badding, A.M. Stacey, L.F. Dahl, J. Am. Chem. Soc. 108 (1986) 3825.

[5] F. Calderoni, F. Demartin, M.C. Iapalucci, G. Longoni, Angew. Chem. Int. Ed. Engl. 35 (1996) 2225.

[6] C. Femoni, M.C. Iapalucci, G. Longoni, P. Svensson, J. Wolowska, Angew. Chem. Int. Ed. Engl. 39 (2000) 1635.

[7] C. Femoni, M.C. Iapalucci, G. Longoni, P. Svensson, Chem. Commun. 8 (2000) 655.

[8] A. Ceriotti, N. Masciocchi, P. Macchi, G. Longoni, Angew. Chem. Int. Ed. Engl. 38 (1999) 3724.

[9] N.T. Tran, M. Kawano, D.B. Powell, R.K. Hayashi, C.F. Campana, L.F. Dahl, J. Am. Chem. Soc. 121 (1999) 5945.

[10] F. Demartin, C. Femoni, M.C. Iapalucci, G. Longoni, P. Zanello, J. Cluster Sci., in press.

[11] J.M. Bemis, L.F. Dahl, J. Am. Chem. Soc. 119 (1997) 4545.

[12] K. Masaki, J.W. Bacon, C.F. Campana, L.F. Dahl, J. Am. Chem. Soc. 118 (1996) 7869.

[13] N.T. Tran, M. Kawano, D.B. Powell, L.F. Dahl, J. Am. Chem. Soc. 120 (1998) 10986.

[14] G. Longoni, C. Femoni, M.C. Iapalucci, P. Zanello, in: P. Braunstein, L. Oro, P. Raithby (Eds.), Metal Clusters in Chemistry, vol. II, VCH, Weinheim, 1999, p. 1137.

[15] F. Fabrizi de Biani, C. Femoni, M.C. Iapalucci, G. Longoni, P. Zanello, A. Ceriotti, Inorg. Chem. 38 (1999) 3721.

[16] J. Sinzig, L.J. de Jongh, A. Ceriotti, R. Della Pergola, G. Longoni, M. Stener, K. Albert, N. Rosch, Phys. Rev. Lett. 81 (1998) 3211.

[17] A. Ceriotti, F. Demartin, G. Longoni, M. Manassero, G. Piva, G. Piro, M. Sansoni, B.T. Heaton, J. Organomet. Chem. 301 (1986) C5.

[18] R. Della Pergola, L. Garlaschelli, F. Demartin, M. Manassero, N. Masciocchi, G. Longoni, J. Chem. Soc. Dalton Trans. (1988) 201.

[19] R.W. Broach, L.F. Dahl, G. Longoni, P. Chini, A.J. Schultz, J.M. Williams, Adv. Chem. Ser. 167 (1978) 93.

[20] J.V. Barkley, B.T. Heaton, L. Manzi, A.K. Smith, A. Steiner, H. Nakayama, K. Miyagi, R. Harding, T. Eguchi, G. Longoni, J. Organomet. Chem. 573 (1999) 254.

[21] A. Ceriotti, P. Chini, R. Della Pergola, G. Longoni, Inorg. Chem. 22 (1983) 1595.

[22] A. Fumagalli, S. Martinengo, G. Ciani, A. Sironi, J. Chem. Soc. Chem. Commun. (1983) 453.

[23] D. Braga, K. Henrick, B.F.G. Johnson, J. Lewis, M. McPartlin, W.J.H. Nelson, A. Sironi, M.D. Vargas, J. Chem. Soc. Chem. Commun. (1983) 1131.

[24] V.G. Albano, D. Braga, G. Ciani, S. Martinengo, J. Organomet. Chem. 213 (1981) 293.

[25] S. Martinengo, G. Ciani, A. Sironi, J. Am. Chem. Soc. 104 (1982) 328.

[26] N.N. Greenwood, A. Earnshaw, Chemistry of the Elements, Pergamon, Oxford, 1990.

[27] A. Fumagalli, S. Martinengo, G. Ciani, J. Organomet. Chem. 273 (1984) C46.

[28] A. Ceriotti, F. Demartin, B.T. Heaton, P. Ingallina, G. Longoni, M. Manassero, M. Marchionna, N. Masciocchi, J. Chem. Soc. Chem. Commun. (1989) 786.

[29] J.L. Vidal, J.M. Troup, J. Organomet. Chem. 213 (1981) 351.

[30] V.G. Albano, F. Demartin, C. Femoni, M.C. Iapalucci, G. Longoni, M. Monari, P. Zanello, J. Organomet. Chem. 593–594 (2000) 325.

[31] C.E. Briant, R.G. Smith, D.M.P. Mingos, J. Chem. Soc. Chem. Commun. (1984) 586.

[32] S. Martinengo, A. Fumagalli, R. Bonfichi, G. Ciani, G. Marturan, Inorg. Chem. 25 (1986) 592.

[33] (a) R. Della Pergola, F. Demartin, L. Garlaschelli, M. Manassero, S. Martinengo, N. Masciocchi, D. Strumolo, Inorg. Chem. 30 (1991) 846. (b) R. Della Pergola, F. Cea, L. Garlaschelli, N. Masciocchi, M. Sansoni, J. Chem. Soc. Dalton Trans. (1994) 1501.

[34] J.C. Calabrese, L.F. Dahl, P. Chini, G. Longoni, S. Martinengo, J. Am. Chem. Soc. 96 (1974) 2614.

[35] D.A. Nagaki, L.D. Lower, G. Longoni, P. Chini, L.F. Dahl, Organometallics 5 (1986) 1764.

[36] J.L. Vidal, W.E. Walker, R.L. Pruett, R.C. Schoening, Inorg. Chem. 18 (1979) 129.

[37] D. Imhof, L.M. Venanzi, Chem. Soc. Rev. (1994) 185.

[38] J.C. Calabrese, L.F. Dahl, A. Cavalieri, P. Chini, G. Longoni, S. Martinengo, J. Am. Chem. Soc. 96 (1974) 2616.

[39] L. Bengtsson-Kloo, M.C. Iapalucci, G. Longoni, S. Ulvenlund, Inorg. Chem. 37 (1998) 4335.

[40] C. Mealli, D.M. Proserpio, J. Chem. Educ. 67 (1990) 399.

[41] A. Ceriotti, G. Longoni, G. Piva, Inorg. Synth. 26 (1989) 312.

[42] G.M. Sheldrick, SADABS, Univerity of Gottingen, Germany.

[43] A. Altomare, G. Cascarano, C. Giacovazzo, A. Guagliardi, M.C. Burla, G. Polidori, M. Camalli, J. Appl. Crystallogr. 24 (1994) 435.

[44] G.M. Sheldrick, SHELX-97, University of Gottingen, Germany.